

TESLA NOTE Feb 4, 1993

A Reduced Bunch Charge Parameter Set for TESLA

H. Padamsee and K. Berkelman
 Laboratory of Nuclear Studies, Cornell University, Ithaca, NY 14853
 and
 A. Mosnier, CEN, Saclay

1. Introduction

One of the problems with the baseline TESLA 500 parameter set is that backgrounds are not as good as the newest parameter set for NLC. This is mostly due to the high bunch charge. If energy degradations and photon induced backgrounds are not kept low, an e+e- collider will have no compelling advantage over a pp collider. To remedy the higher background problem, we examine the consequences of a reduced bunch charge. As we show in section 2, this has very good consequences for the background.

Since luminosity lost scales as N^2 , we re-gain part of the luminosity by reducing the final focus spot size from 100 nm to 64 nm. The new spot size is still larger than the design goal of the Final Focus Test Facility at SLAC. We keep the starting emittances the same. The collision frequency is increased from 8 kHz to 19 KHz by doubling the number of bunches from 800 to 1600, and increasing the rep rate from 10 to 11.9 Hz. Up to now, the number of bunches (800) was limited by the minimum spacing (7m) between bunches and a ring the size of HERA (6 km). At the Garmisch workshop, Delahaye proposed a scheme to reduce the spacing between bunches in the damping ring by a factor of 8. So it should be possible to double the number of bunches.

One disadvantage of increasing the number of bunches is that the RF pulse would have to be twice as long, and this becomes expensive for the refrigerator associated capital and operating cost. To bring this component back within the realm of the baseline TESLA 500 parameters, we propose to decrease the bunch spacing by a factor of 2. This of course impacts the multi-bunch instability situation, which is examined carefully in section 3. The bottom line is that because of the reduced bunch charge the stability situation is actually somewhat improved.

Table 1 compares the two parameter sets. For NLC and DLC the parameters used are from those summarized by Greg Loew at the Garmisch LC92 Workshop.

2. Backgrounds

All background calculations are done with techniques discussed in [1].

Fig. 1 shows the scaled luminosity spectra for e+e- and $\gamma\gamma$ versus the scaled effective center-of-mass energy squared, $z = s/s_{max} = E_1 \times E_2 / E_0^2$. Results for the baseline and new TESLA 500 parameter sets are compared. Since e+e- cross sections contain the factor $1/E^2$, experiments at the maximum energy tend to be rate limited. Reduction in luminosity at the highest energy is a serious limitation on the physics potential of a collider. So it is the luminosity at the peak energy that really counts. In this respect, the new parameter set is a factor of 2 improvement. Fig. 2 compares the differential luminosity with DLC and the new

NLC parameter list. It is clear that the old TESLA baseline parameter set needs the improvement provided by the new set.

The luminosity tail will produce events at lower center of mass energies. The $1/E^2$ dependence of the cross section enhances the effect of the luminosity tail. If the tail is large, there is a danger that the experiment will be swamped with uninteresting low energy events, degrading the physics productivity of the high energy experiment. Fig. 3 compares the tails for the different machines and old and new TESLA parameter sets. The new TESLA parameter set is the best.

Fig. 3 is a comparison of the integral luminosity spectra for the various machines.

[1] K. Berkelman, CLIC Note 154, 164

Table 1

Parameter	Units	NLC	DLC	Old TESLA	NEW TESLA
Emittance x	$\mu\text{m-rad}$	5	10	20	20
Emittance y	$\mu\text{m-rad}$	0.05	1	1	1
beta* x	mm	10	5	10	6
beta *y	mm	0.1	0.8	5	2
σ_x	nm	300	316	640	495
σ_y	nm	3	40	101	64
σ_z	μm	100	500	1000	1000
Υ		0.1	0.09	0.07	0.04
Dy		8	8.5	7.9	8
δE		0.03	0.05	0.03	0.014
Luminosity	10^{33}	6	2.2	5	5.1
AC Power.....	MW	152	145	137	154
$N \times 10^{10}$		0.65	2.2	5.14	2.5
f _c	Khz	16.2	8.6	8	19
Number of bunches		90	172	800	1600
Rep rate	Hz	180	50	10	11.9
Bunch spacing	μsec	0.0014	0.011	1	0.5
RF Freq	GHz	11.4	3	1.3	1.3
Beam Power	MW	8.4	15	33	38
Refrigerator	kw	0	0	58	59
Peak Power/m	MW/m	13	12.2	0.2	0.2
Gradient	MV/m	50	17	25	25

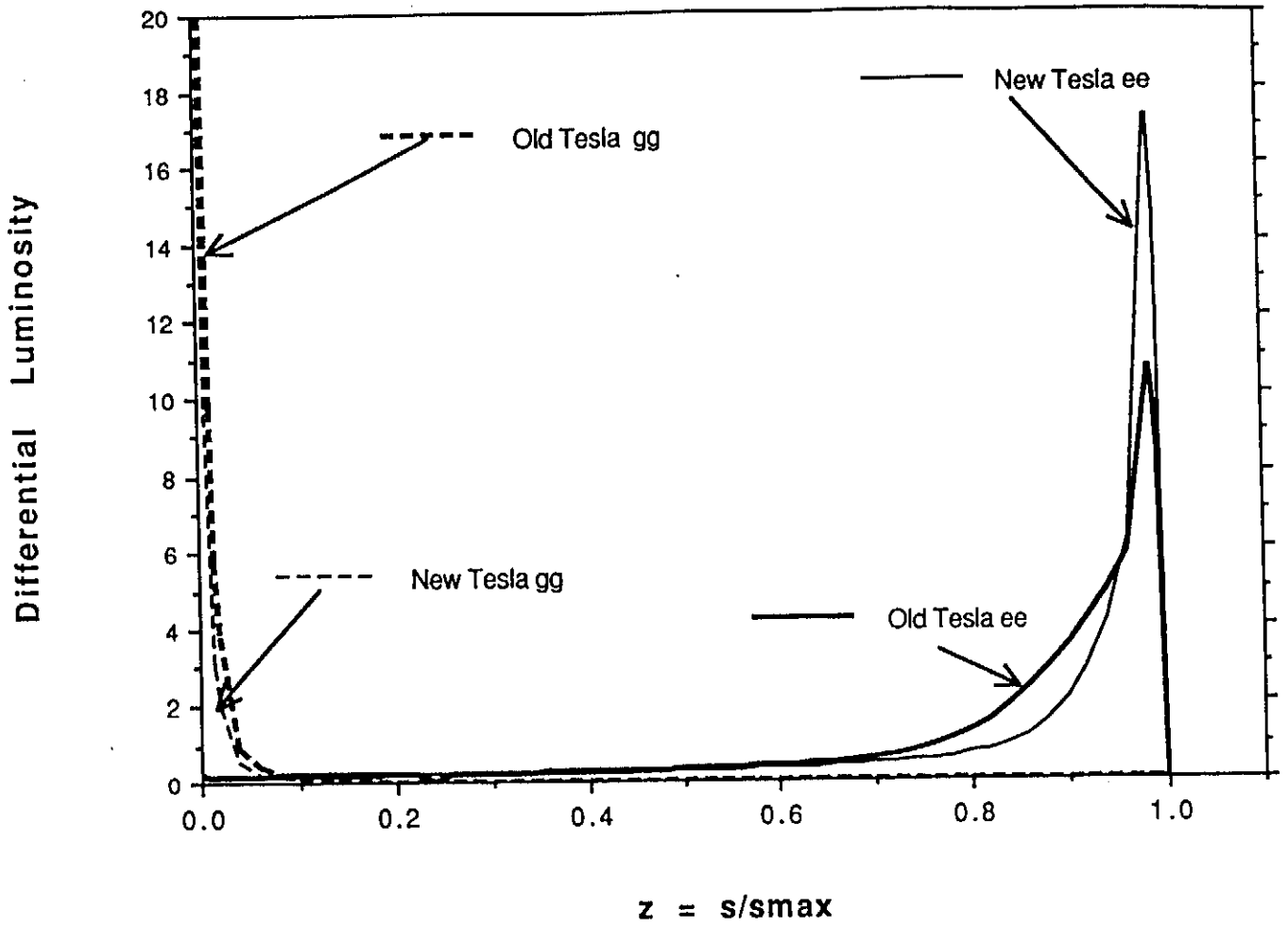


Fig 1

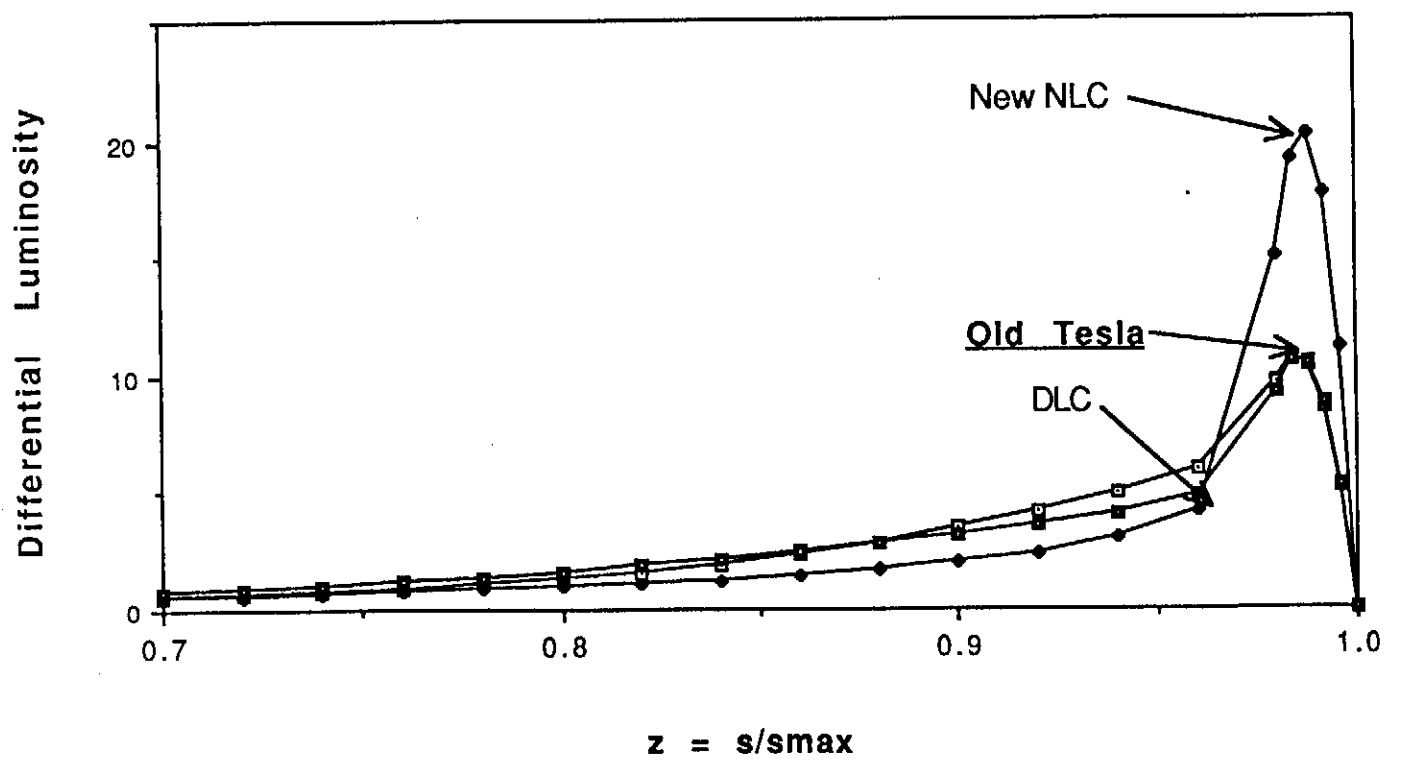
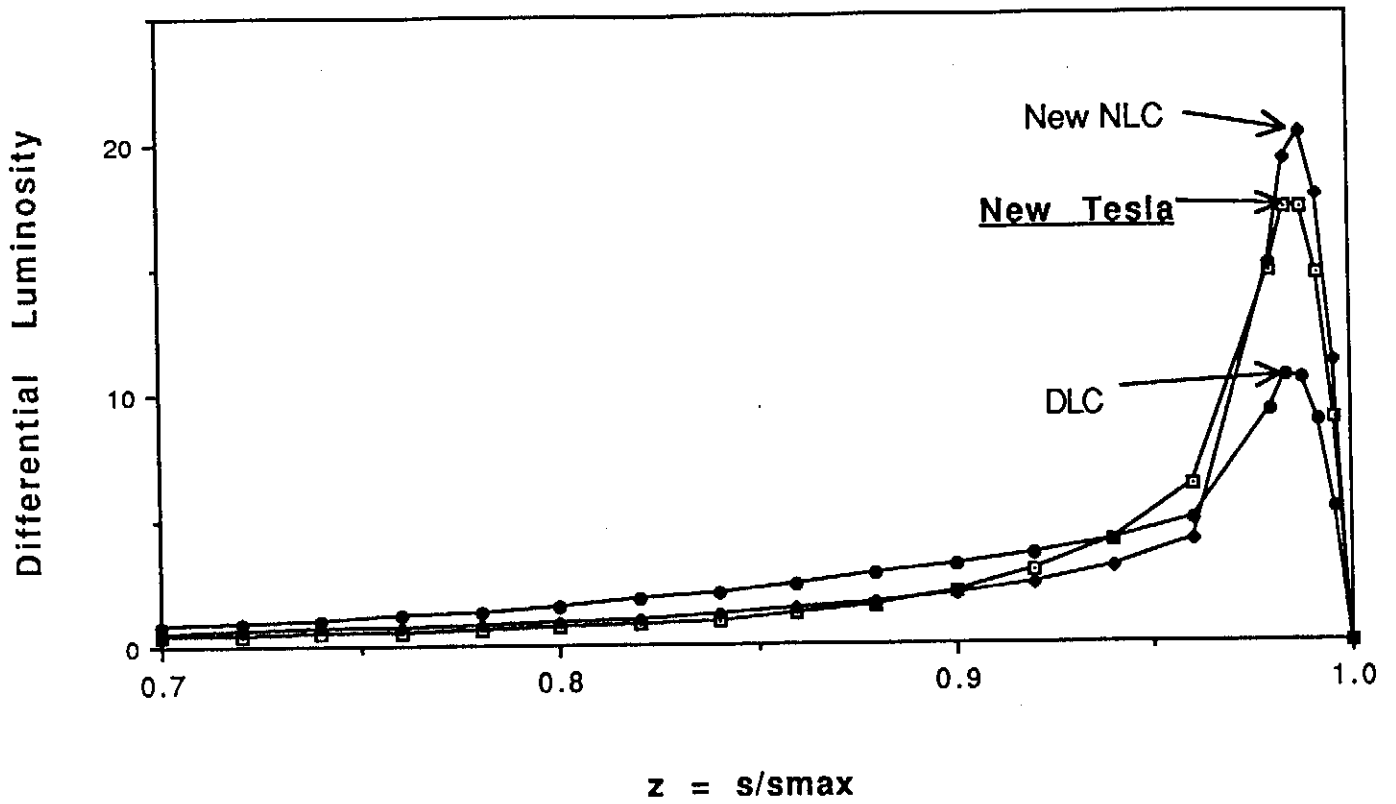


Fig 2

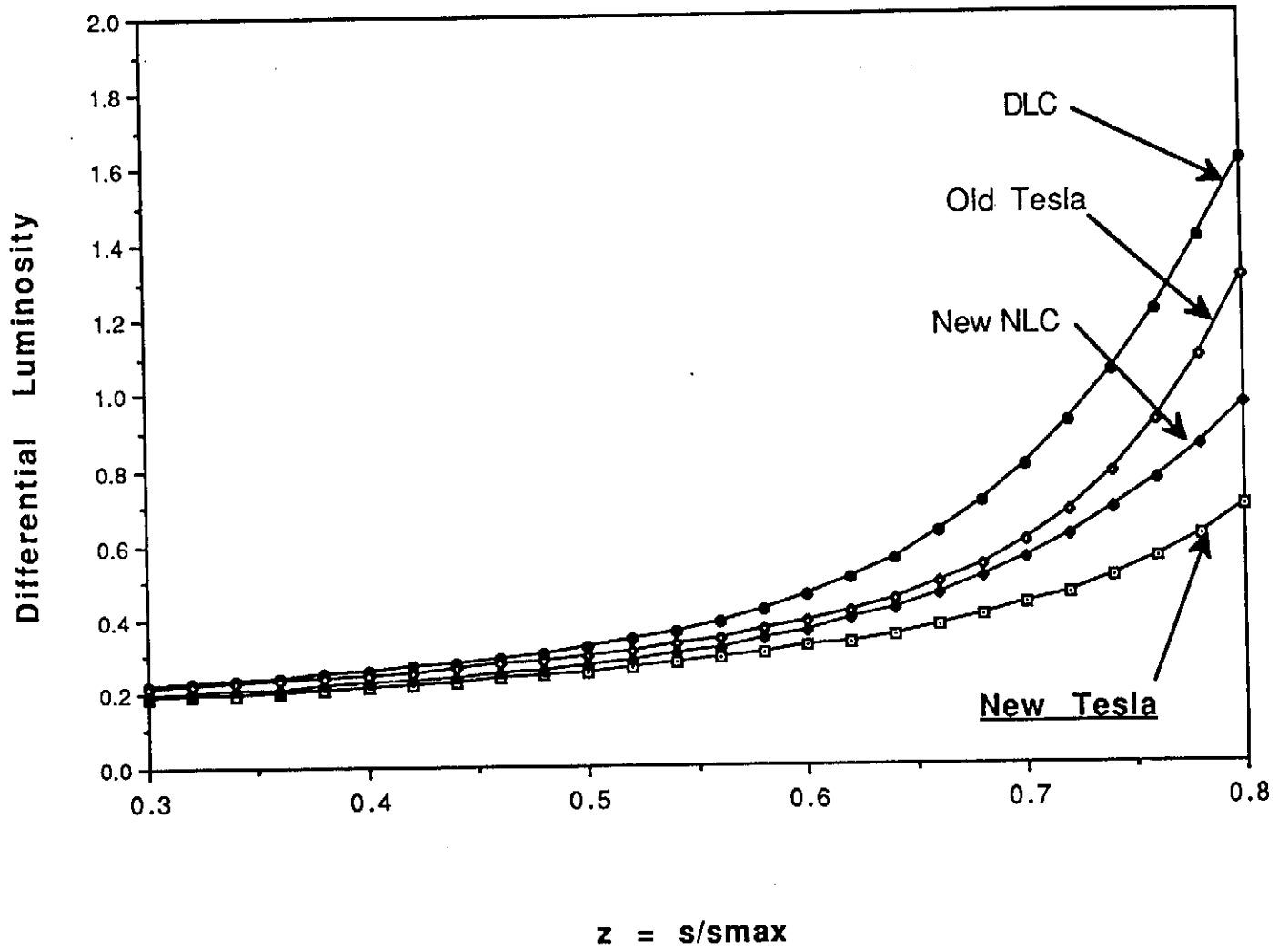


FIG. 3

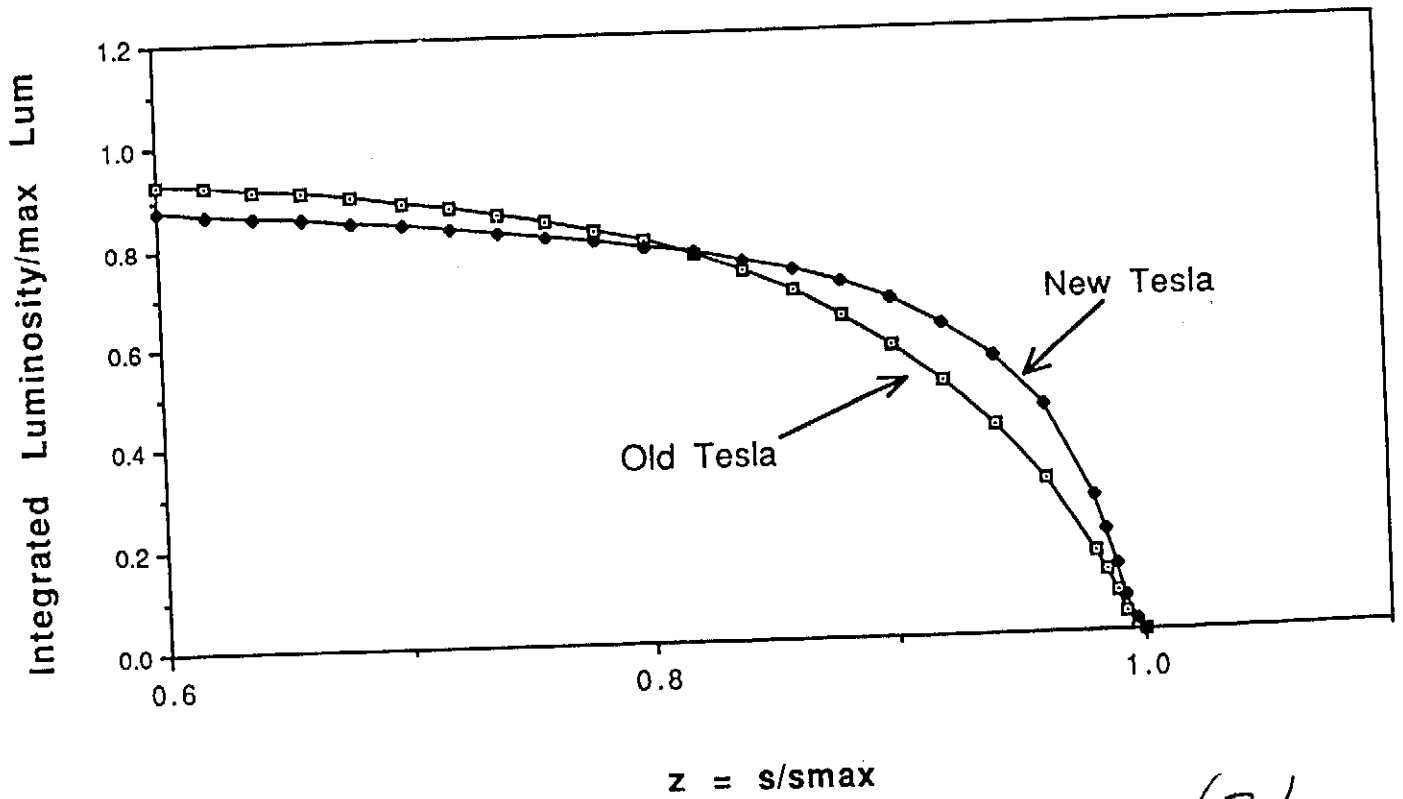
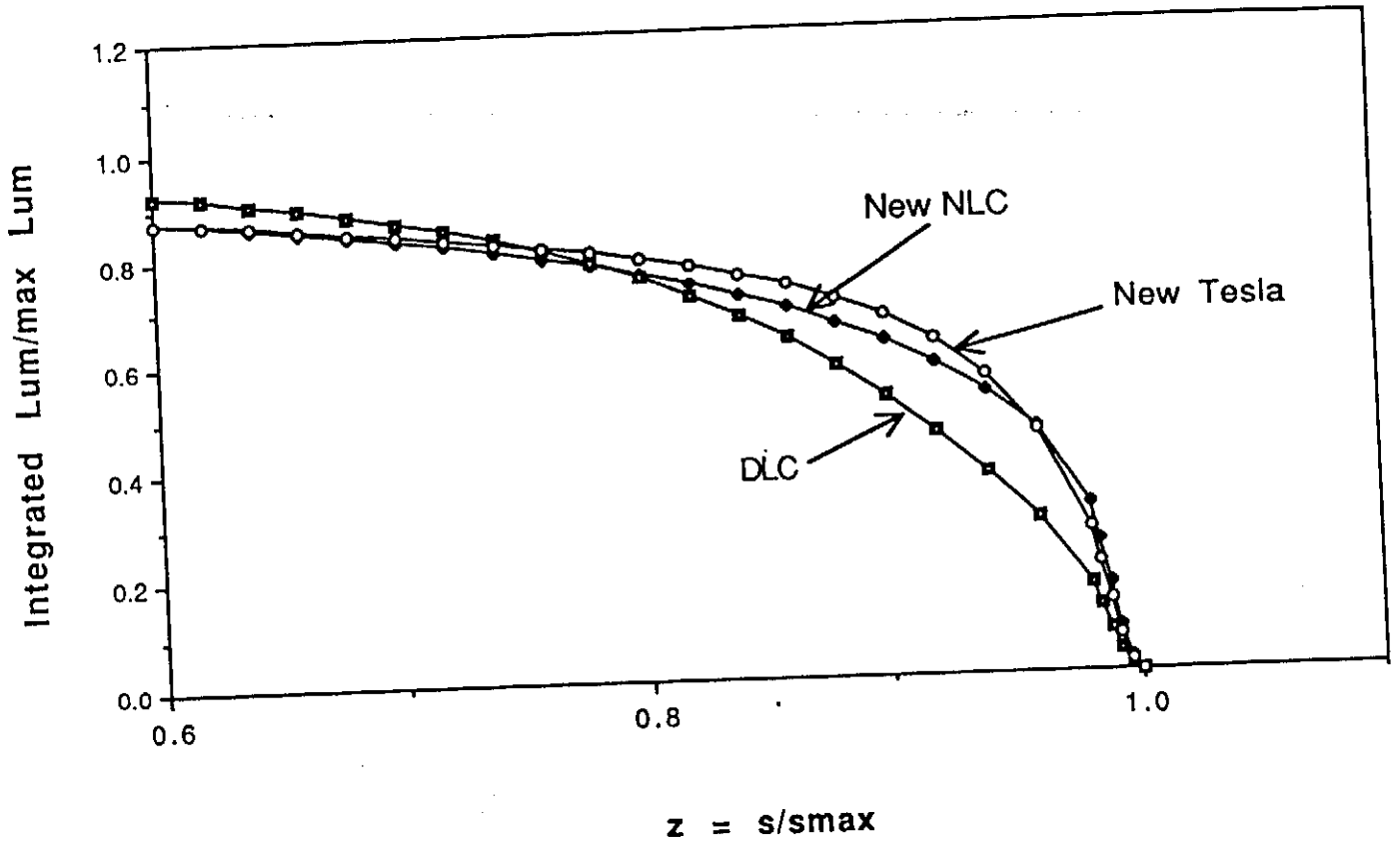


FIG. 4

(71)

3. Beam Dynamics in the Linac

The preservation of beam emittances during the transport through the linac is essential to achieve maximum luminosity. Transverse emittance degradation occurs when beam trajectories are displaced from the accelerator components axis : chromatic effects due to the finite energy spread are generated by the focussing magnets while beam instabilities due to the excitation of wakefields are induced by the accelerating structures. Given a maximal allowed emittance growth, these effects assess the alignment tolerances for the quadrupoles and the cavities. Estimations of the emittance growths for the first set of parameters are given in [1]. It was concluded that cavity and quadrupole scatters of respectively 500 and 100 μm result in a maximum emittance growth of 20 % when the constant beta and phase advance FODO lattice is optimized simultaneously for chromatic and single bunch wakefield effects. The optimal beta value was found about 66 m, corresponding to 24 cavities between two adjacent quadrupoles. With this lattice and taking the first ten modes of highest impedance with their predicted loaded Q's, multi-bunch instability calculations showed a maximum emittance growth of 2 % with a cavity scatter of 1 mm. We carry out now the same study with the new parameter set : a lower emittance dilution is expected in the single bunch case because the bunch charge is reduced but the multi-bunch case is not so clear since the bunch spacing is also reduced. In addition, results on different lattice types where beta is not constant but energy dependent are also given.

Moreover tiny - random or correlated - vibrations of the magnets due to ground motion dilute the emittance. Vibration tolerances are given for the constant beta lattice and the square root of energy beta scaling scheme. Since only single particle dynamics is involved (no wakes), the results are common to both sets of parameters.

Single Bunch Instabilities

First the energy spread of the bunch, induced by the rf wave curvature and the longitudinal wake, is minimized by proper choice of the linac phase. The bunch charge being reduced, the wake is weaker and the optimal phase shift with respect to the wave crest is smaller. Table 1 gives the rf phase and the resulting rms energy spread for both sets of parameters with cuts at $\pm 3\sigma$ of the bunch distribution. Figure 1 shows the energy profiles for the new set when only the wake effect, only the rf curvature effect and both effects are taken into account.

Parameter set	Old	New
Optimal rf phase	3°	1.5°
rms energy spread (10^{-4})	5.5	3.8

Table 1

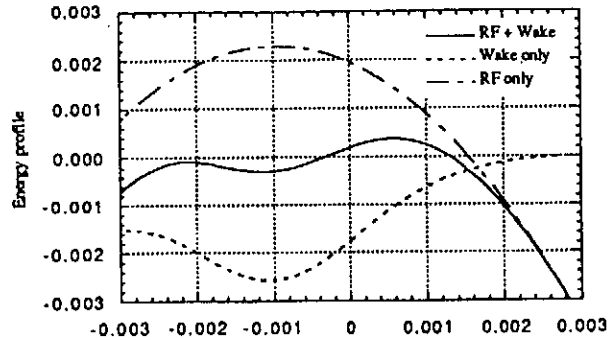


Figure 1 : Energy profiles (bunchlength 1 mm and bunch population $2.5 \cdot 10^{10}$)

The emittance at the end of the linac is then calculated with a computer code, which tracks the slice centroids and sigma matrices of the slices of a bunch divided in 41 slices. The longitudinal bunch wake and transverse wake potentials of the cavity are identical to the ones used in [1]. We assume the same cavity ($500 \mu\text{m}$) and quadrupole ($100 \mu\text{m}$) alignment scatters. The classical one to one trajectory correction is also used with a beam position monitor error of $50 \mu\text{m}$ relative to the quadrupole center.

The constant beta FODO lattice

In the case of a constant beta FODO lattice, the cell length - and hence the beta value - is varied to try to find a balance between the chromatic and the wakefield effects. In order to get proper statistics, the simulations are repeated with at least 20 different seeds of the random errors generator. The vertical emittance growths for different number of cavities per half cell are showed in figure 2 and 3 for the bunch charges of respectively 5 and $2.5 \cdot 10^{10}$. In both cases, the optimal average beta value is about 66 m, but as expected, the dilution is nearly 4 times smaller for the new parameter set.

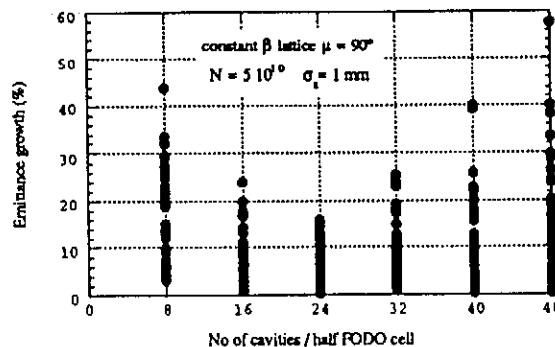


Figure 2 : Emittance growth (%) vs number of cavities / half cell (bunch population = $5 \cdot 10^{10}$)

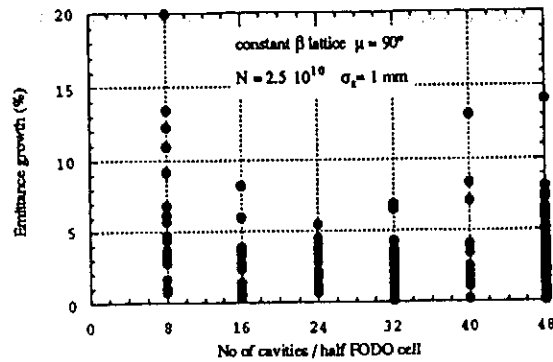


Figure 3 : Emittance growth (%) vs number of cavities / half cell
(bunch population = $2.5 \cdot 10^{10}$)

The \sqrt{E} beta scaling FODO lattice

The emittance growth for the new set of parameters is also computed for another focalisation type : the lattice with the $E^{1/2}$ beta scaling, suggested in [2] because it provides a BNS damping criterion independent of energy. A number of eight cavities per cryomodule is assumed. The modules are then grouped in sections with matching cells in between such that the beta function fits at best the $E^{1/2}$ law. The resulting beta function and the exact scaling are showed in figure 4 for starting cells filled with one cryomodule.

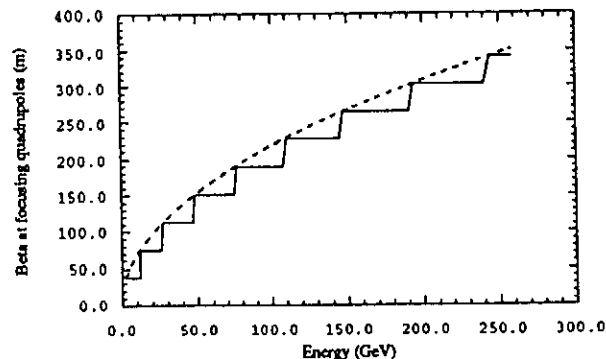


Figure 4 : Beta function for the actual scaling (full line) and for the exact scaling law (dashed line) at the focusing quadrupoles.

The matching cells are assumed perfect without any error. We found for this lattice a maximal emittance growth of 7 % among 20 calculations with different seeds. Concerning the single bunch instability, we can conclude that this lattice and the optimized constant beta lattice give nearly the same emittance dilution.

Multi-bunch Instabilities

The bunches are now treated as macroparticles and are tracked through the 10000 cavities. The rms emittance is calculated at the exit of the linac from the bunch phase space coordinates. Like in [1] the ten cavity modes of highest impedance are selected. The cavity are misaligned with $\sigma_{\text{offset}}=1$ mm and the mode frequency spread is $\sigma_{\text{freq}}=1$ MHz. The simulations are again repeated with at least 20 different seeds.

The constant beta FODO lattice

The normalized emittances for different number of cavities per half cell are showed for the two sets of parameters in figures 5 and 6. We conclude that for the bunch charge of $2.5 \cdot 10^{10}$, despite the doubling of both the number of bunches and the arrival frequency, the dilution due to the multi-bunch effect is slightly lower than for the bunch charge of $5 \cdot 10^{10}$. For a beta value of about 66 m, the rms emittance is below 2 % of the vertical design value.

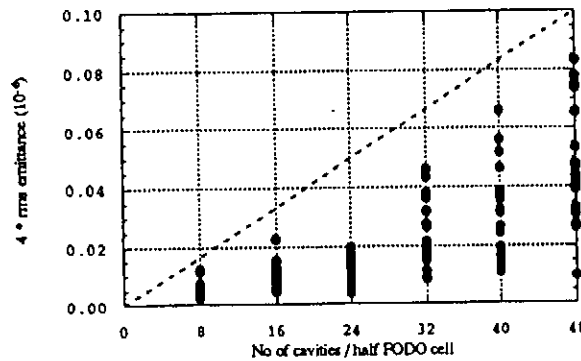


Figure 5 : rms normalized emittance vs number of cavities / half cell (bunch population = $5 \cdot 10^{10}$, bunch spacing = $1 \mu\text{S}$, train of 800 bunches)

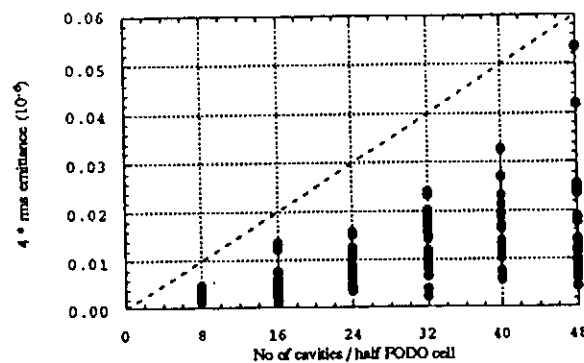


Figure 6 : rms normalized emittance vs number of cavities / half cell (bunch population = $2.5 \cdot 10^{10}$, bunch spacing = $0.5 \mu\text{S}$, train of 1600 bunches)

The \sqrt{E} beta scaling FODO lattice

The multi-bunch instability for the new set of parameters is also computed with the focalisation of figure 4. Very high emittances are found with a maximum of $13 \cdot 10^{-6}$ among 20 computations with different seeds. We conclude that the instability induced by wakefields is better controlled with a constant FODO lattice. This is confirmed by inspecting the emittance evolutions along the linac for both focalisation types in figure 7. While the emittance is kept constant after a quick increase at the beginning in the constant beta case ($\beta = 66 \text{ m}$), the emittance is continuously growing in the non constant beta case (starting $\beta = 22 \text{ m}$).

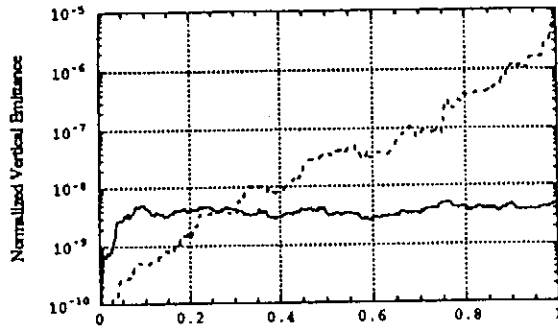


Figure 7 : Emittance evolutions along the linac for the constant beta (full line) and the $E^{1/2}$ beta scaling (dashed line) FODO lattices.

If we look at lattices with beta functions of different energy dependences

$$\beta = \beta_0 \left(\frac{\gamma}{\gamma_0} \right)^\alpha \quad \text{and phase advance} = 90^\circ$$

we verify the rapid increase of the emittance with the power α (figure 8), when the focalisation strength is progressively relaxed

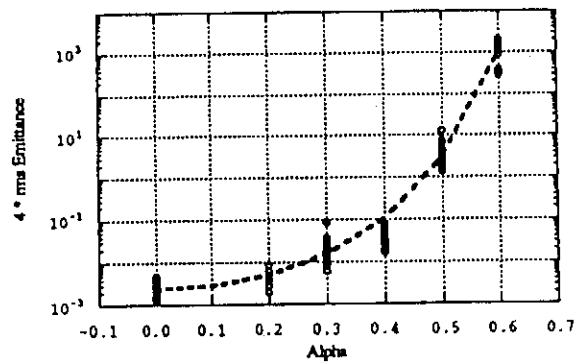


Figure 8 : rms emittances for different E^α beta scaling lattices.

Vibration Tolerances

We consider first an uncorrelated motion of quadrupoles. The beam trajectory is deflected by every off-axis magnet and the beam displacement at the exit of the linac is the sum of the betatron oscillations excited by the misaligned quadrupoles [2]

$$y_f = \sum_{n=0}^{N_q-1} \frac{d_n}{f_n} \sqrt{\beta_f \beta_n} \sqrt{\gamma_n / \gamma_f} \sin(\psi_f - \psi_n) \quad (1)$$

where d_n , f_n are the displacement and the focal length of the n th quadrupole and β_n is the beta value at the quadrupole location and Ψ is the phase advance of the lattice. Assuming random errors, the quadratic average of the beam displacement is

$$\langle y_f^2 \rangle = \sum_{n=0}^{N_q-1} \frac{\langle d^2 \rangle}{2} \frac{\beta_f \beta_n}{f_n^2} \frac{\gamma_n}{\gamma_f}$$

Performing the sum for a large number of quadrupoles, the beam response to a random jitter of motion amplitude d_{rms} is approximately for both constant beta and $E^{1/2}$ beta scaling lattices given by (see reference [2], [3] or [4])

$$\frac{y_{f,rms}}{d_{rms}} = \frac{\sqrt{N_q}}{\cos \mu / 2}$$

where μ is the phase advance per cell. If we limit the beam jitter to one quarter of the beam size at the exit (emittance growth of about 6 %) the amplitude of the quadrupole motion must be then lower than 100 nm for the constant beta case and 200 nm for the \sqrt{E} beta scaling case.

We consider now correlated quadrupole motion. Following the procedure given in [3] to estimate the beam response for a constant beta lattice, we consider a ground wave shaking the quadrupoles. The displacement of magnet n is then

$$d_n = \hat{d} \cos \left(2 \pi n \frac{L_c}{\lambda_g} + \phi \right)$$

where L_c is the cell length, λ_g is the ground wavelength and ϕ is the initial phase shift. The sum of equation (1) is now performed on the focusing and defocusing quadrupoles :

$$y_f = \frac{\hat{d} \sqrt{\beta_f}}{f_0} \left[\sqrt{\beta_F} \sum_n \cos(k_g n L_c + \phi) \sin(\psi_f - n \mu) \sqrt{\gamma_n / \gamma_f} \right. \\ \left. - \sqrt{\beta_D} \sum_n \cos(k_g (n+1/2) L_c + \phi) \sin(\psi_f - (n+1/2) \mu) \sqrt{\gamma_{n+1/2} / \gamma_f} \right]$$

where β_F and β_D are the beta functions at focusing and defocusing quadrupoles locations.

Using simple trigonometric relations and eliminating the rapidly varying terms, we note that there is coherent build-up if the following relation is fulfilled

$$k_g L_c \pm \mu = 2 p \pi \quad \text{or} \quad \frac{\lambda_\beta}{\lambda_g} \pm 1 = \frac{2 p \pi}{\mu}$$

The beam displacement at the exit of the linac is

$$y_f = \pm \frac{\hat{d} \sqrt{\beta_f}}{2 f_0} \left(\sqrt{\beta_F} - (-1)^p \sqrt{\beta_D} \right) \sin(\pm \psi_f + \phi) \sum_n \sqrt{\gamma_n / \gamma_f}$$

and the rms beam response is then

$$\frac{y_b}{\hat{d}} = \frac{\sqrt{\beta_f}}{3 \sqrt{2} f_0} \left(\sqrt{\beta_F} - (-1)^p \sqrt{\beta_D} \right) N_{\text{cell}}$$

For the TESLA parameters, the phase advance per cell is 90° and the cell length is about 66 m. The first and second resonances appear for $\lambda_\beta = \lambda_g$ and $\lambda_\beta = 3 \lambda_g$ (ground wave frequencies of 1.1 and 3.4 Hz assuming phase velocity of 300 m/s), where the response values are respectively 100 and 250. This is reproduced by figure 9, which shows the beam response versus the oscillation frequency, computed from tracking simulations with oscillating magnets. These simulations confirm the large peak values exhibited by a constant beta lattice.

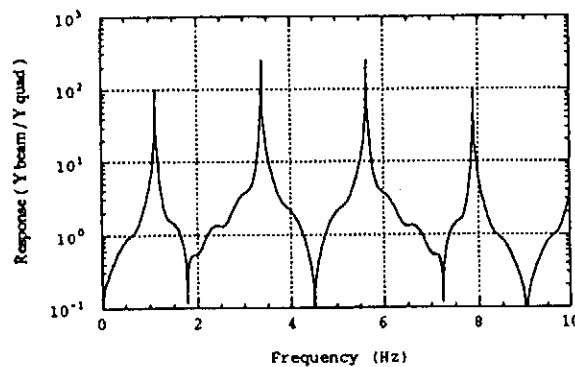


Figure 9 : rms beam response to a correlated quadrupole motion in case of constant beta lattice

If we limit for the highest resonance, the beam jitter to one quarter of the beam size at the exit, as for the uncorrelated case, the wave amplitude must be lower than 11 nm at the resonance frequency.

Figure 10 shows the computed beam response for the nearly $E^{1/2}$ beta scaling lattice of figure 4. Moderate resonance peaks appear above 0.5 Hz and the highest peaks below 2 Hz can be identified as the first (quoted peaks 1 and 2) and second resonances (quoted peaks 3 and 4) excited by the last constant beta sections of the linac. It is clear that the constraints on the vibration amplitudes are stronger for the constant beta case, but the beam feedback electronics can be narrow-band and hence more efficient [5].

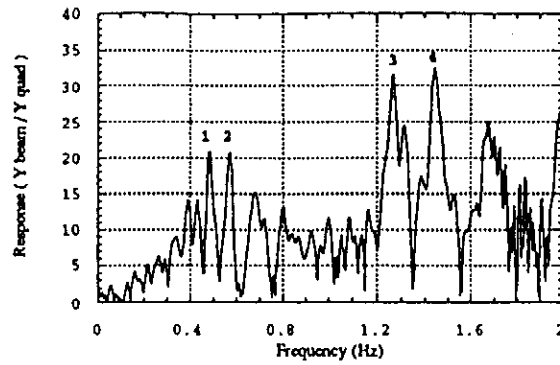


Figure 10 : rms beam response to a correlated quadrupole motion in case of the $E^{1/2}$ beta scaling lattice.

References

- [1] A. Mosnier, O. Napoly, "Wakefield effects in a Superconductin Linear Collider", HEACC Hamburg, 1992.
- [2] R. Ruth, Frontier of Particle Beams 296, Springer-Verlag, 1986
- [3] T.O. Raubenheimer, "The generation and acceleration of low emittance flat beams for future linear colliders", SLAC-Report-387, Nov. 1991
- [4] A. Mosnier, internal report, DAPNIA-SEA-91-16
- [5] T.O. Raubenheimer, unpublished, Linear Collider Workshop 1992 (Garmish)